Requirement for epithelial p38α in KRAS-driven lung tumor progression

Jessica Vitos-Faleato[a], Sebastián M. Real[a], Nuria Gutierrez-Prat[a], Alberto Villanueva[b], Elisabet Llonch[a], Matthias Drosten[c], Mariano Barbacid[c], and Angel R. Nebreda[a,d,1]

[a]Institute for Research in Biomedicine, The Barcelona Institute of Science and Technology, 08028 Barcelona, Spain; [b]Program Against Cancer Therapeutic Resistance, Catalan Institute of Oncology, Bellvitge Institute for Biomedical Research, 08907 L'Hospitalet de Llobregat, Spain; [c]Molecular Oncology Program, Centro Nacional de Investigaciones Oncológicas, 28029 Madrid, Spain; and [d]Institució Catalana de Recerca i Estudis Avançats (ICREA), 08010 Barcelona, Spain

Edited by Melanie H. Cobb, University of Texas Southwestern Medical Center, Dallas, TX, and approved December 29, 2019 (received for review December 9, 2019)

Malignant transformation entails important changes in the control of cell proliferation through the rewiring of selected signaling pathways. Cancer cells then become very dependent on the proper function of those pathways, and their inhibition offers therapeutic opportunities. Here we identify the stress kinase p38α as a nononcogenic signaling molecule that enables the progression of $Kras^{G12V}$-driven lung cancer. We demonstrate in vivo that, despite acting as a tumor suppressor in healthy alveolar progenitor cells, p38α contributes to the proliferation and malignization of lung cancer epithelial cells. We show that high expression levels of p38α correlate with poor survival in lung adenocarcinoma patients, and that genetic or chemical inhibition of p38α halts tumor growth in lung cancer mouse models. Moreover, we reveal a lung cancer epithelial cell-autonomous function for p38α promoting the expression of TIMP-1, which in turn stimulates cell proliferation in an autocrine manner. Altogether, our results suggest that epithelial p38α promotes $Kras^{G12V}$-driven lung cancer progression via maintenance of cellular self-growth stimulatory signals.

lung adenocarcinoma | KRAS | nononcogene addiction | p38α | TIMP-1

Despite the many efforts invested during recent decades, the development of selective therapies remains one of the biggest challenges in oncology. Nowadays, lung adenocarcinomas in advanced stages, like those driven by mutations in EGFR or ALK, are often treated with tyrosine kinase inhibitors, but, unfortunately, tumors tend to become resistant in less than 1 y and continue to progress (1, 2). The development of targeted therapies for KRAS-induced lung tumors has proven especially difficult. Most of the mutated KRAS forms lack suitable pockets to which drugs can bind in order to interfere with the oncogenic function, and targeting some of the downstream kinases leads to undesirable toxicities (3). An alternative approach consists of targeting synthetic lethal partners of the mutated KRAS so that cancer cells have their viability compromised, while the normal cells without the mutated driver gene are not affected. When these partners do not have oncogenic activity themselves, the exacerbated dependency on the cancer cell for their function has been termed "nononcogene addiction" (4). This is the case for the transcription factor GATA2, whose deletion induces the regression of established KRAS mutant lung tumors in mice (5). Therefore, charting a comprehensive map of nononcogene addictions in KRAS-driven cancer may help to develop new therapies.

The protein kinase p38α, also known as mitogen-activated protein kinase (MAPK) 14, is normally stimulated by environmental stresses and other cues, orchestrating cell responses like proliferation, differentiation, or apoptosis depending on the stimulus and the cell type (6, 7). In the tumor context, p38α has been shown to interfere with malignant cell transformation in different tissues (8–10). In particular, p38α has been reported to suppress lung tumor formation, a function that is probably related to its ability to induce the differentiation of progenitor cells (9). Curiously, no functionally significant genomic alterations for p38α have been described in tumors, and there is evidence that p38α might be constitutively phosphorylated in several cancer types (11–13). In fact, immunohistochemistry and phosphoproteomic analysis have reported phosphorylated p38α in the tumors from non–small-cell lung carcinoma (NSCLC) patients (14–16). Both the scarcity of inactivating mutations and the presence of phosphorylated p38α in tumors suggest the possibility that cancer cells may use this nononcogenic signaling pathway to facilitate tumor progression. Consistent with this notion, epithelial cancer cells in the intestine have been shown to exploit p38α for colon tumor maintenance in vivo (10). However, whether p38α in epithelial cancer cells of other tissues contributes to tumor progression remains to be explored. Indeed, it is important to contextualize the outcomes of p38α inhibition in the different cell types of a tissue as well as the global effect of its ubiquitous down-regulation given that the complex regulation of survival/death signals by p38 MAPKs can result in opposite molecular functions during tumor development, as has been reported in UV-induced skin papillomas (17, 18) or in pancreatic ductal adenocarcinomas (19, 20). There is evidence that p38α in stromal cells can support lung tumorigenesis (21) and facilitate metastatic lung cell extravasation (22), but the contribution of p38α signaling in lung cancer epithelial cells to tumor maintenance and progression has not been investigated yet to the authors' knowledge.

Significance

Nearly half of the cases of lung cancer bear mutations in the RAS pathway. Unfortunately, no specific drugs are available to successfully target many RAS-driven tumors that are not surgically resectable. Despite the sound rationale for targeting oncogene products for cancer therapeutics, this often leads to development of resistance. As an alternative, nononcogenic proteins can sometimes facilitate tumor progression, and, even though they are neither mutated nor overexpressed in the malignant cells, they may represent potential targets for anticancer therapies. We have found that nononcogenic signaling through p38α plays a tumor-promoting function in lung adenocarcinoma epithelial cells by inducing the expression of TIMP-1, a growth factor-like protein. We propose that p38α inhibition could be therapeutically useful.

Author contributions: J.V.-F. and A.R.N. designed research; J.V.-F., S.M.R., N.G.-P., and E.L. performed research; A.V., M.D., and M.B. contributed new reagents/analytic tools; J.V.-F. and A.R.N. analyzed data; and J.V.-F. and A.R.N. wrote the paper.

The authors declare no competing interest.

This article is a PNAS Direct Submission.

Published under the PNAS license.

[1]To whom correspondence may be addressed. Email: angel.nebreda@irbbarcelona.org.

This article contains supporting information online at https://www.pnas.org/lookup/suppl/doi:10.1073/pnas.1921404117/-/DCSupplemental.

First published January 22, 2020.

In this study, we have used mouse models of $Kras^{G12V}$-driven lung cancer and spheroid cultures of lung cancer cells to show a tumor-promoting role of epithelial p38α in established lung tumors.

Results

p38α Expression Correlates with Malignancy and Poor Prognosis in Lung Adenocarcinoma Patients. To investigate the role of p38α in lung cancer, we first analyzed the expression levels of the *MAPK14* gene (encoding p38α) in a cohort of lung adenocarcinoma patients, formed by 107 tumor samples in stages I to IV. The levels of *MAPK14* mRNA were significantly increased in the tumors in comparison to the paired normal parenchyma (Fig. 1*A*). Next, in two other different cohorts of 293 and 138 samples of tumors in stages I to III with patient follow-up data, we observed that, irrespective of the tumor stage, the highest level of *MAPK14* expression correlated with a higher mortality rate (Fig. 1*B*), as well as with a shorter time to relapse in lung adenocarcinoma patients both in general (Fig. 1*C*) and in Kras-driven adenocarcinoma cohorts (*SI Appendix*, Fig. S1 *A* and *B*). To confirm the results obtained by analyzing public mRNA datasets, we used antibodies against phosphorylated p38 or total p38α to stain a human tissue microarray, which contained samples of lung adenocarcinomas and paired adjacent normal lung tissue, as well as normal lung tissue from patients without tumors. In line with the mRNA analysis, we observed that lung tumors contained a higher number of both phosphorylated p38- and p38α-positive cells than the normal lung parenchyma (Fig. 1 *D* and *E*).

In parallel, we used mice expressing $Kras^{+/FSFG12V}$, which develop lung adenocarcinomas upon intratracheal administration of adenoviruses expressing FlpO recombinase (23). Immunohistochemistry analysis confirmed a significantly increased phospho-p38 staining in $Kras^{G12V}$-driven lung tumors compared to the healthy parenchyma (Fig. 1*F*), supporting our observations in the lung adenocarcinoma-patient cohorts. Altogether, these results hint at the implication of p38α in lung cancer, and suggest that its expression levels could be used as an independent prognostic factor for lung adenocarcinoma.

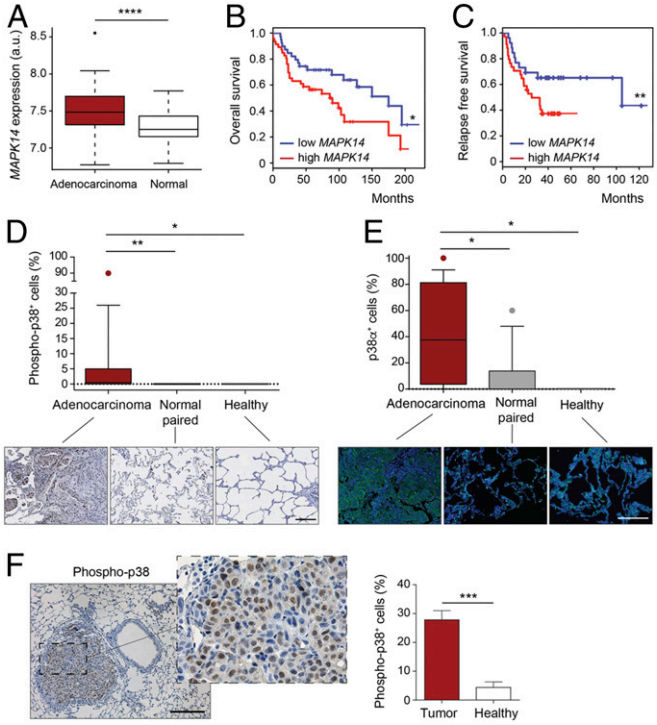

Fig. 1. High levels of p38α expression correlate with malignancy and poor prognosis. (*A*) Boxplots for expression levels of *MAPK14* mRNA comparing paired adenocarcinomas and healthy tissues ($n \geq 49$ per group). a.u., arbitrary units. (*B*) Kaplan–Meier plots showing a univariate analysis of overall survival of lung adenocarcinoma patients stratified by high or low *MAPK14* mRNA expression ($n \geq 39$ per group). (*C*) Kaplan–Meier plots displaying a recurrence-free survival over time of lung adenocarcinoma patients stratified by high or low *MAPK14* mRNA expression ($n \geq 26$ per group). (*D*) Representative images and boxplot of the percentage of phospho-p38$^+$ cells in lung adenocarcinoma tumors ($n = 17$), paired normal tissue ($n = 14$), and healthy lung parenchyma ($n = 5$) from a human tissue array. (Scale bar, 200 μm.) (*E*) The same samples as in *D* were stained with a p38α antibody by immunofluorescence. DAPI marks nuclei. (*F*) Representative image of a murine $Kras^{G12V}$-driven lung tumor stained with phospho-p38 antibody. (Scale bar, 200 μm.) The histogram shows the percentage of phospho-p38$^+$ cells in tumors and in healthy lung parenchyma ($n = 5$ healthy tissues and $n = 21$ tumors from 6 different mice). Data represent average ± SEM. *$P < 0.05$, **$P < 0.01$, ***$P < 0.001$, ****$P < 0.0001$.

Down-Regulation of p38α in Alveolar Epithelial Progenitor Cells Enhances $Kras^{G12V}$ Lung Tumorigenesis but Compromises Tumor Progression. The correlation between *MAPK14* (p38α) expression and lung tumor malignancy was unexpected, given that p38α down-regulation has been reported to sensitize lung tissue to $Kras^{G12V}$-induced oncogenic transformation (9). When mice have p38α ubiquitously down-regulated, they exhibit uncontrolled proliferation of the alveolar epithelial type II (AE2) progenitor cells (8, 9), which can function as lung adenocarcinoma initiating cells (24, 25). However, since tumor-associated stromal cells can also regulate tumorigenesis, we investigated the role of p38α particularly in the alveolar progenitor cells during lung tumor development. To address this, we induced $Kras^{G12V}$ expression in lungs of mice carrying $Mapk14^{lox/lox}$ alleles and the surfactant protein C (SPC)-Cre-ER transgene, in which *Mapk14* can be specifically deleted in AE2 cells (Fig. 2*A* and *SI Appendix*, Fig. S1*C*). When these mice were treated with tamoxifen, we observed a 25% down-regulation of the floxed exon 2 of *Mapk14* in AE2 progenitor cells both by qRT-PCR (*SI Appendix*, Fig. S1*D*) and by using a double-fluorescent Cre reporter (*SI Appendix*, Fig. S1*E*). Consistently, 20 wk after $Kras^{G12V}$ expression, mice with AE2 cell-specific down-regulation of p38α (p38α-Δ^{SPC}) showed numerous lung tumors constituted by SPC$^+$ cells growing along the preexisting alveolar framework. The p38α-Δ^{SPC} tumors showed a significantly increased percentage of proliferative cells, as marked by Ki67 staining, compared to their wild-type (WT) counterparts (Fig. 2*B*). We also observed an increased lung weight in p38α-Δ^{SPC};$Kras^{G12V}$ mice (*SI Appendix*, Fig. S1*F*), as well as enhanced recruitment of immune cells in their lungs (Fig. 2*C*), which correlated with increased STAT3 phosphorylation (*SI Appendix*, Fig. S1*G*), a well-known mediator of tumor-promoting inflammation. Accordingly, p38α-Δ^{SPC} mice showed increased lung tumor burden (Fig. 2*D*). Taken together, these results support a tumor-suppressor role of p38α in AE2 progenitor cells of the lung epithelia.

Surprisingly, the increased lung tumor burden observed in $Kras^{G12V}$-expressing p38α-Δ^{SPC} mice correlated with a higher percentage of early-stage hyperplasias versus adenomas compared with the tumors in $Kras^{G12V}$-expressing WT mice, in which there were more adenomas than hyperplasias (Fig. 2*E*). These observations suggest that p38α down-regulation facilitates tumor initiation, but, once the lung epithelial cells are transformed, the absence of p38α delays tumor progression to more advanced stages, hinting at a possible tumor-promoting role for p38α in lung cancer cells.

p38α Promotes $Kras^{G12V}$-Driven Lung Tumor Growth. If p38α is required for lung tumor progression, the acute loss of p38α in established tumors would be expected to hinder tumor growth. To test this hypothesis, we first looked at the effect of the ubiquitous down-regulation of p38α using p38α-Δ^{Ub} mice, which bear $Mapk14^{lox/lox}$ alleles and the tamoxifen-inducible ubiquitin

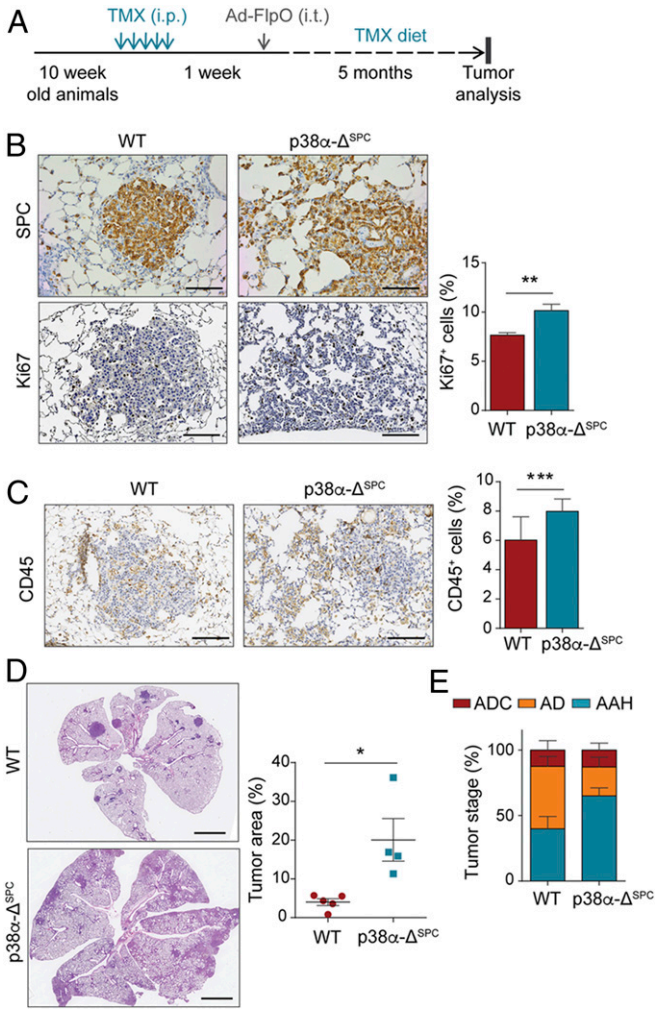

Fig. 2. p38α-Δ^{SPC} mice show increased tumor burden but delayed progression to advanced stages. (*A*) Schematic representation of the experimental treatment regimen. Ad-FlpO, adenovirus expressing FlpO recombinase; TMX, tamoxifen; i.p., intraperitoneal injection; i.t., intratracheal administration. (*B*) Representative images of WT and p38α-Δ^{SPC} lungs stained for the AE2 marker SPC or with Ki67 antibody to detect proliferative cells. (Scale bars, 100 μm.) The histogram shows the quantification of the percentage of Ki67$^+$ cells per tumor ($n = 50$ WT and $n = 47$ p38α-Δ^{SPC} tumors from 5 different mice each). (*C*) Representative images of WT and p38α-Δ^{SPC} lungs stained with CD45 antibody to estimate the degree of immune cell infiltration. (Scale bars, 100 μm.) The histogram shows the quantification of the CD45$^+$ area as a percentage of the total area analyzed ($n = 30$ WT and $n = 56$ p38α-Δ^{SPC} tumors from 3 different mice each). (*D*) Representative images of WT and p38α-Δ^{SPC} lungs stained with H&E. Dot plots show the quantification of the tumor area ($n \geq 4$ mice). (Scale bars, 2 mm.) (*E*) Tumors were microscopically analyzed and classified according to their pathological stage as adenocarcinoma (ADC), adenoma (AD), and atypical adenomatous hyperplasia (AAH; $n \geq 4$ mice). Data represent average ± SEM. *$P < 0.05$, **$P < 0.01$, ***$P < 0.001$.

C (UBC)-Cre-ERT2 transgene. The efficiency of p38α down-regulation was confirmed by immunoblotting and PCR in both whole-lung lysates and individual tumors (Fig. 3*A* and *SI Appendix*, Fig. S2 *A* and *B*). It is noteworthy that the levels of both total p38α and phosphorylated p38 were higher in lungs expressing oncogenic Kras^{G12V} than in healthy lung tissue (Fig. 3*A*). Therefore, we induced Kras^{G12V} expression, confirmed the presence of lung tumors 20 wk later, and then induced p38α down-regulation (Fig. 3*B*). Interestingly, the down-regulation of p38α resulted in a significantly decreased number and size of macroscopic lung tumors in comparison to the tamoxifen-treated WT mice (*Mapk14*$^{lox/lox}$ without UBC-Cre-ERT2; Fig. 3*C*). Indeed, the number and size of lung tumors in p38α-Δ^{Ub} mice were similar to those in animals analyzed at the initial time point, prior to tamoxifen injections, suggesting that p38α down-regulation produced a cytostatic effect. In contrast, WT animals treated with tamoxifen showed a substantial increase in both the number of tumors and the average tumor size in comparison to the animals analyzed before p38α down-regulation (Fig. 3*C*). This indicates that tamoxifen by itself does not interfere with lung tumor growth. As an additional control, we performed the same experiment using mice bearing UBC-Cre-ERT2 and *Mapk14*$^{+/+}$ alleles and found no significant differences upon tamoxifen treatment between WT mice and the *Mapk14*$^{+/+}$;UBC-Cre-ERT2 control group in lung tumor number or in size, ruling out any effect related to the Cre recombinase activity by itself (*SI Appendix*, Fig. S2*C*). Histological analysis of the tumors showed a remarkable decrease in the percentage of advanced lesions in p38α-Δ^{Ub} mice, with adenocarcinomas being decreased threefold (Fig. 3*D*). Collectively, these results further support the decreased ratio of advanced versus early lesions observed in p38α-Δ^{SPC} lungs and suggest that Kras^{G12V}-driven lung tumors are addicted to p38α signaling.

To investigate the cause of the reduced lung tumor load observed upon p38α down-regulation, we performed immunohistochemistry analysis of lung sections. We found that infiltrating lymphocytes (CD3$^+$), which remained mainly at the periphery of the tumors, and macrophages (CD68$^+$) were present in similar numbers in WT and p38α-Δ^{Ub} animals. Blood vessel distribution, as determined by CD31$^+$ staining, was also similar in tumors from both groups of mice. Likewise, we detected no differences in the number of apoptotic cells by TUNEL or by cleaved-caspase 3 staining (*SI Appendix*, Fig. S2 *D–F*). However, the number of proliferating cells, as determined by Ki67 immunostaining, was significantly diminished in lung tumors from p38α-Δ^{Ub} mice (Fig. 3*E*). Therefore, the acute loss of p38α in developing lung tumors does not alter the numbers of infiltrating immune cells or the vasculature density, but it impairs cancer cell proliferation and tumor progression to more advanced stages.

Chemical Inhibition of p38α Reduces Lung Tumor Burden in Mice. The dependency of lung tumor progression on p38α is a potentially relevant observation from a clinical perspective. As a proof of principle, we used the low molecular weight chemical compound PH797804 to inhibit the kinase activity of p38α. Mice in which Kras^{G12V} lung tumors had been induced 20 wk before were administered either PH797804 or vehicle solution via oral gavage for 14 d. We found that mice treated with the p38α inhibitor showed a significant decrease in the number and size of lung tumors in comparison to the vehicle-treated group (Fig. 4*A*). Inhibition of p38α signaling in the lungs was confirmed by immunoblotting analysis of phosphorylation of Hsp27, a downstream target of the pathway (Fig. 4*B*). Moreover, we observed that the number and size of lung tumors in mice treated with PH797804 were similar to those found before the treatment, suggesting that p38α inhibition produces a cytostatic effect. In addition, the number of advanced lesions, as well as the percentage of Ki67$^+$ cells per tumor, were significantly reduced (Fig. 4 *C* and *D*). These results mirror our observations in p38α-Δ^{Ub} mice and show that the role of p38α promoting lung tumor progression is mediated through its kinase activity. Moreover, these results suggest that p38α inhibition could be potentially useful for NSCLC therapy.

Epithelial p38α Is Necessary for the Proliferation of Lung Cancer Cells in Anchorage-Independent Conditions. To investigate how p38α contributes to the progression of lung tumors, we tried to induce p38α deletion in epithelial cells using mice bearing SPC-Cre-ER and Kras$^{+/FSFG12V}$ alleles, but, since Cre activity was limited to roughly 25% of the AE2 cells (*SI Appendix*, Fig. S1 *D* and *E*), the level of p38α

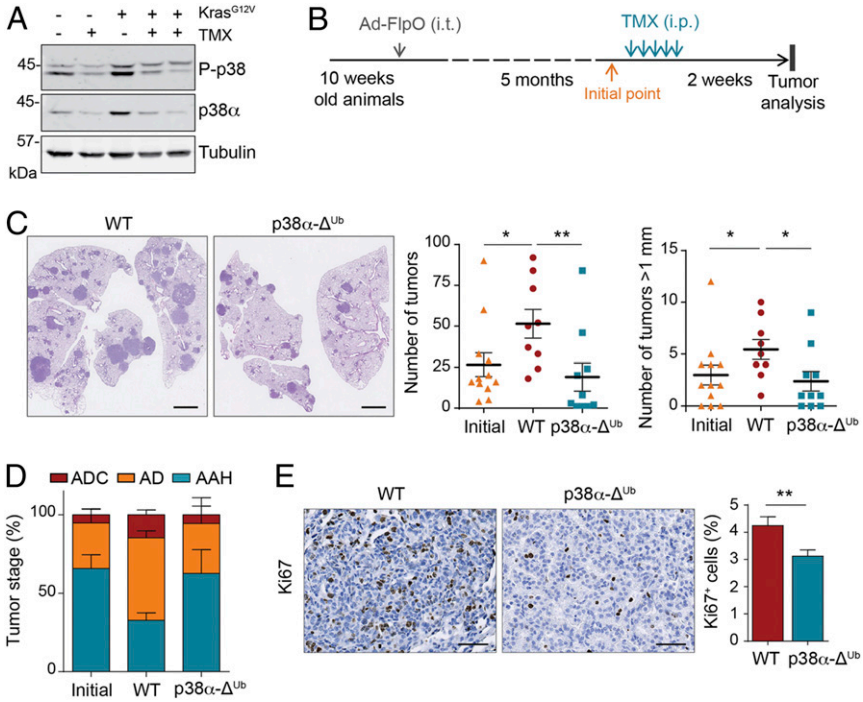

Fig. 3. p38α enables $Kras^{G12V}$-driven lung tumor progression. (*A*) Representative immunoblots with antibodies to p38α and phospho-p38 (P-p38) of whole lung lysates from WT and p38α-deficient mice, as indicated by − and + tamoxifen (TMX), respectively, either expressing or not expressing $Kras^{G12V}$. Tubulin was used as loading control. Each line corresponds to one mouse. (*B*) Schematic representation of the experimental treatment regimen. Ad-FlpO, adenovirus expressing FlpO recombinase; i.p., intraperitoneal injection; i.t., intratracheal administration. (*C*) Representative images of WT and p38α-Δ^{Ub} lungs stained with H&E. (Scale bars, 2 mm.) Dot plots show the quantification of both the tumor number and the number of tumors bigger than 1 mm in diameter per animal before (initial) and 2 wk after the TMX treatment in WT and p38α-Δ^{Ub} mice ($n \geq 9$ mice per group). (*D*) Tumors as in *C* were microscopically analyzed and classified according to their pathological stage as adenocarcinoma (ADC), adenoma (AD), and atypical adenomatous hyperplasia (AAH; $n \geq 6$ mice per group). (*E*) Representative images of WT and p38α-Δ^{Ub} lungs collected 1 wk after TMX injections and stained with Ki67 antibody to detect proliferative cells. (Scale bars, 100 μm.) The histogram shows the quantification of $Ki67^+$ cells as a percentage of the total number of cells counted per tumor ($n = 37$ WT and $n = 27$ p38α-Δ^{Ub} tumors from 3 different mice each). Data represent average ± SEM. $^*P < 0.05$, $^{**}P < 0.01$.

knocked-down cells in the tumors was insufficient to draw conclusions. Therefore, to study the role of p38α in malignant lung epithelial cells, we established ex vivo cultures of cancer cells (named mKLC) isolated from murine $Kras^{G12V}$ lung adenocarcinomas (26). We used mice with *Mapk14*$^{lox/lox}$ alleles so that *Mapk14* can be deleted in the mKLC cells upon Cre recombinase expression to generate p38α-deficient cells (p38α-Δ^{mKLC}). We confirmed that mKLC cells expressed the EpCAM epithelial marker and retained E-cadherin expression upon p38α down-regulation (*SI Appendix*, Fig. S3 *A* and *B*). We first looked at the proliferation capacity of the mKLC cells in vitro. Strikingly, we observed no differences in their cell cycle or their ability to incorporate 5-bromo-2′-deoxyuridine (BrdU) when cultured in standard monolayer conditions (*SI Appendix*, Fig. S3 *C* and *D*). Similarly, Lewis lung carcinoma (LLC1) murine cells with p38α down-regulated by shRNAs showed no differences with WT cells in BrdU incorporation (*SI Appendix*, Fig. S3 *E* and *F*) and had no growth advantage when injected s.c. into the rare flanks of nude mice (*SI Appendix*, Fig. S3*G*).

Interestingly, when mKLC cells were cultured in soft agar to mimic tumor growth, we observed that WT and p38α-Δ^{mKLC} cells formed a similar number of colonies after 20 d in culture but p38α-Δ^{mKLC} colonies were significantly smaller (Fig. 5*A*). In a complementary experiment, we noticed that inducing the down-regulation of p38α in established colonies formed by mKLC cells slowed down their growth (*SI Appendix*, Fig. S3*H*). These results were confirmed using H358 human lung cancer cells, which also formed smaller colonies in soft agar in the presence of two different p38α chemical inhibitors (*SI Appendix*, Fig. S3*I*).

Consistent with these observations, both WT and p38α-Δ^{mKLC} cells intratracheally implanted in immunocompetent mice formed a similar number of lung tumors (Fig. 5 *B* and *C*). However, tumors formed by p38α-Δ^{mKLC} cells showed a significantly decreased size and less proliferative cells (Fig. 5 *C* and *D*). Likewise, we implanted mKLC cells expressing Cre-ERT2 intratracheally into C57BL/6 mice and, once lung tumors were formed, p38α down-regulation was induced in vivo. We found that p38α down-regulation significantly diminished the number and size of the lung tumors (Fig. 5*E*), phenocopying the results observed using the UBC-Cre-ERT2;$Kras^{+/FSFG12V}$ mice. Importantly, these data indicate that the proliferation assays in 2D cell cultures and s.c. xenografts do not reproduce the in vivo scenario in lung tumors upon p38α down-regulation. Instead, p38α signaling appears to have an important contribution to the proliferation of $Kras^{G12V}$-driven epithelial lung cancer cells when these cells are challenged by culturing in anchorage-independent conditions or by orthotopic implantation in mice.

To further understand the role of p38α in lung tumor progression, we investigated the effect of p38α depletion on the metastatic features of mKLC cells. We found that both WT and p38α-deficient cells showed equivalent adhesion and migration capacities, resistance to anoikis, and extravasation abilities (*SI Appendix*, Fig. S4 *A*–*D*). We next confirmed these results by implanting WT and p38α-Δ^{mKLC} cells into the rare flanks of immunodeficient mice. The number of lung metastatic foci detected 2 wk after primary tumor resection was similar in both groups, indicating a similar ability of p38α-Δ^{mKLC} and WT cells to disseminate and colonize the lung (*SI Appendix*, Fig. S4*E*). However, when we injected LLC1 cells through the tail vein of

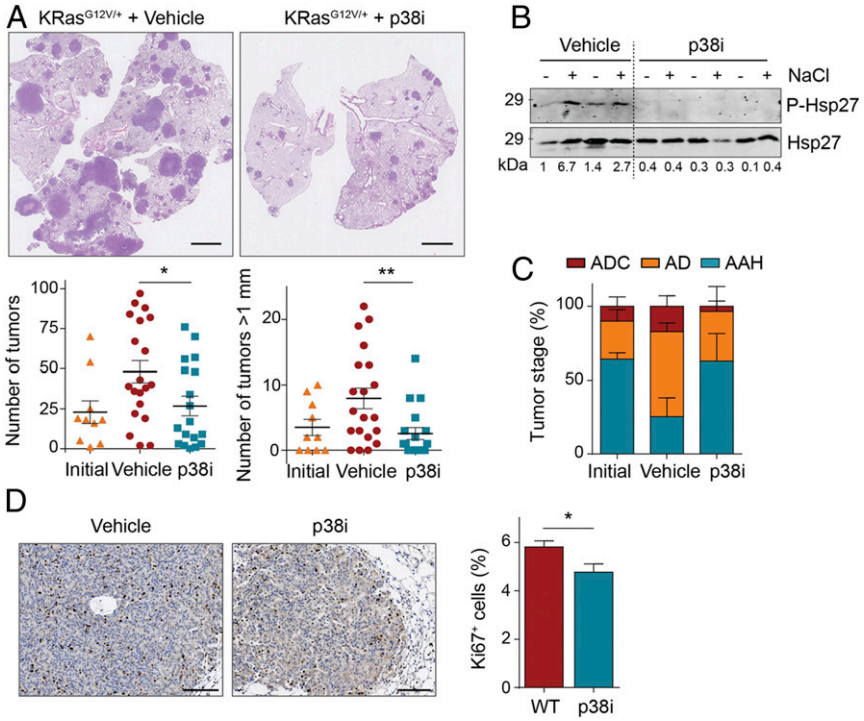

Fig. 4. Chemical inhibition of p38α impairs the growth of Kras^{G12V}-driven lung adenocarcinomas. (*A*) Representative images of H&E-stained lungs from animals treated with vehicle or the p38α inhibitor PH797804 (p38i). (Scale bars, 2 mm.) Dot plots show the quantification of both the tumor number and the number of tumors bigger than 1 mm in diameter per animal before (initial) and after 2 wk of treatment with vehicle or p38i ($n \geq 10$ mice per group). (*B*) Lungs with tumors from Kras^{G12V}-expressing animals that were administered vehicle or p38i for 15 d, were treated with NaCl ex vivo to hyperactivate the p38α pathway or left untreated, and then were immunoblotted with the indicated antibodies. Each pair of lines (–, +) corresponds to one mouse. Representative examples are shown. (*C*) Tumors were microscopically analyzed and classified according to their pathological stage as adenocarcinoma (ADC), adenoma (AD), and atypical adenomatous hyperplasia (AAH; $n = 3$ mice). (*D*) Representative images of lung tumors from animals treated with vehicle or p38i for 15 d that were stained with Ki67 antibody to detect proliferative cells. (Scale bars, 100 μm.) The histogram shows the quantification of Ki67$^+$ cells per tumor as a percentage of the total number of cells counted ($n = 70$ vehicle- and $n = 33$ p38i-treated tumors from 4 different mice each). Data represent average ± SEM. $^*P < 0.05$, $^{**}P < 0.01$.

nude mice, 2 wk later, we observed a smaller lung tumor burden in animals injected with p38α-deficient cells (*SI Appendix*, Fig. S4*F*). The difference in lung tumor area but not in metastatic dissemination ability suggests that p38α does not impact on the metastatic properties of the epithelial lung cancer cells, but mainly affects their proliferation rate and hence the tumor mass growth rate.

p38α-Mediated Expression of TIMP-1 Induces Lung Cancer Cell Proliferation. There is evidence that p38α can regulate both the expression of cytokines and the transducing signaling pathways engaged by these factors, which can stimulate cancer cell proliferation (11). Therefore, we analyzed the possibility that secreted factors controlled by p38α could self-stimulate the proliferation of lung cancer cells. We used an antibody array to check the expression of 40 cytokines in lung tumors formed by the orthotopic inoculation of either WT or p38α-Δ^{mKLC} cells, and validated the results in individual tumors by qRT-PCR (*SI Appendix*, Fig. S5 *A*–*C*). We identified TIMP-1 as one of the most significantly down-regulated cytokines (Fig. 6*A*). Moreover, p38α down-regulation in lung tumors resulted in decreased levels of *Timp1* mRNA (Fig. 6*B*). Accordingly, TIMP-1 protein levels in p38α-deficient mouse lungs, either healthy or bearing Kras^{G12V}-driven tumors, were decreased in comparison to the equivalent WT lungs (Fig. 6*C*).

TIMP-1 is an inhibitor of matrix metalloproteinases that can also promote lung tumor growth through its binding to CD63 (27), and is usually expressed at high levels in lung cancer patients with poor prognosis (28, 29). Hence, we investigated whether the reduced *Timp1* expression was responsible for the impaired proliferation of p38α-deficient lung cancer cells. First, we analyzed *Timp1* mRNA levels in epithelial cancer cells sorted from mouse lung tumors, and observed that *Timp1* expression was dependent on p38α (*SI Appendix*, Fig. S5*D*). We also obtained evidence of TIMP-1 implication in epithelial lung cancer cell proliferation by using two different TIMP-1 shRNAs, which reduced the size of colonies formed by mKLC cells grown in soft agar, an effect that was attenuated in the presence of recombinant TIMP-1 (Fig. 6 *D* and *E*). Moreover, the addition of recombinant TIMP-1 also rescued the decreased colony size observed in p38α-deficient mKLC cells grown in soft agar (Fig. 6*F*). Similar results were observed by adding recombinant TIMP-1 to human H460 and murine mKLC cells treated with p38α chemical inhibitors (Fig. 6*G* and *SI Appendix*, Fig. S5*E*). Interestingly, analysis of public gene expression databases revealed a direct correlation between the expression of *Timp1* and *MAPK14* mRNAs in human adenocarcinomas (*SI Appendix*, Fig. S5*F*). Therefore, the proliferation of lung cancer epithelial cells is regulated by the levels of TIMP-1, which, in turn, are controlled by p38α.

In fact, the p38α regulated transcription factors AP-1 and ATF-2 have binding sites on the *Timp1* promoter, which also contains two NFκB binding sites (30), and the NFκB pathway has been shown to control TIMP-1 levels in a mouse lung cancer model (27). Since TIMP-1 expression controls lung cancer cell proliferation (Fig. 6*E*), we hypothesized that inhibition of NFκB signaling would phenocopy p38α inhibition. Treatment of soft agar colonies formed by mKLC cells with an inhibitor of IKK2, a

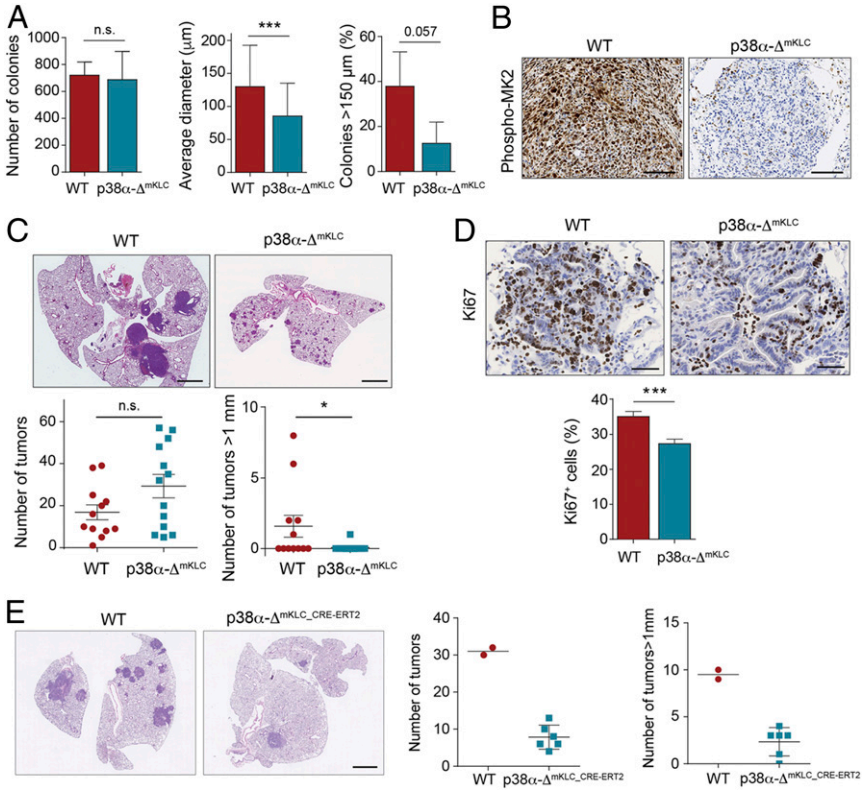

Fig. 5. Epithelial p38α is necessary for the proliferation of lung tumor cells. (*A*) WT and p38α-Δ^{mKLC} cells derived from mouse lung tumors were seeded in soft agar. Histograms show the number of colonies formed, their average diameter, and the percentage of colonies bigger than 150 μm per well ($n \geq 42$ colonies analyzed). Data represent mean ± SD. (*B*) Representative images of phospho-MK2 immunostainings of lung tumors formed by intratracheal inoculation of WT and p38α-Δ^{mKLC} cells. (Scale bars, 100 μm.) (*C*) Representative images of H&E stained lungs from WT animals that were intratracheally inoculated with either WT or p38α-Δ^{mKLC} cells. (Scale bars, 2 mm.) Dot plots show the average number of total tumors and the number of tumors with a diameter bigger than 1 mm at 22 d after the intratracheal inoculation ($n \geq 12$ mice per group). Data represent average ± SEM. (*D*) Representative images of lung tumors from mice that were intratracheally inoculated with either WT or p38α-Δ^{mKLC} cells and stained with Ki67 antibody. (Scale bars, 100 μm.) The histogram shows the quantification of Ki67$^+$ cells per tumor as a percentage of the total number of cells counted ($n = 55$ WT and $n = 70$ p38α-Δ^{mKLC} tumors each from ≥5 mice). Data represent average ± SEM. (*E*) Representative examples of lungs from mice that were intratracheally inoculated with either WT or p38α-$\Delta^{mKLC\_CRE\text{-}ERT2}$ cells and, 22 d later, treated with tamoxifen. Lungs were stained with H&E 15 d after p38α down-regulation. (Scale bar, 2 mm.) Dot plots show the quantification of both the tumor number and the number of tumors bigger than 1 mm in diameter per animal ($n = 2$ to 6 mice). *$P < 0.05$, ***$P < 0.001$. n.s., not significant.

kinase upstream of p65 NFκB, resulted in decreased colony size, which was further decreased by the combined treatment with both p38α and IKK2 inhibitors (*SI Appendix*, Fig. S5*G*). Altogether, these results support a key role for TIMP-1 in Kras-driven lung cancer, indicating that TIMP-1 promotes epithelial lung cancer cell proliferation in an autocrine manner, and that both p38α and NFκB signaling contribute to TIMP-1 production by epithelial cancer cells.

Discussion

Given the plethora of cellular processes that p38α can regulate, its role in tumorigenesis has been hard to define. Depending on the nature of the stimulus, the cell type, and the malignant stage, p38α is involved in cell death or survival, cell cycle entry, or induction of cell differentiation (11, 31). Therefore, it is difficult to predict which tumors could benefit from p38α inhibition without performing in vivo experiments.

Here, we use mouse models of KRAS-driven NSCLC to show that p38α plays a dual role during lung tumorigenesis. We provide evidence that p38α plays a tumor-suppressor function in normal lung epithelial cells, interfering with Kras^{G12V}-driven malignant transformation. In this case, p38α maintains the homeostasis by balancing proliferation and differentiation capacities of alveolar progenitors (9), and maybe also by mediating senescence entry induced by oncogenic Kras expression, as shown in cultured fibroblasts (32, 33). Therefore, in the absence of p38α, there is an increased number of poorly differentiated epithelial cells with the potential to become tumor-initiating cells (9). In addition to the deregulated proliferation of the progenitor cells, p38α-deficient lungs have an enhanced immune response, as indicated by the increased number of CD45$^+$ cells recruited. These immune cells probably belong to the myeloid lineage (8), and collaterally contribute to tumor-promoting inflammation. Despite the benefits that the down-regulation of p38α would entail a priori for tumor development, lung cancer cells do not seem to shut off this anticancer signaling pathway. Instead, we detect increased phosphorylated p38α in lung tumors compared to paired healthy parenchyma, which agrees with previous reports on NSCLC patients (14–16). Moreover, we show that higher p38α levels correlate with poor overall survival and with recurrence in lung adenocarcinoma, as was proposed for colorectal cancer (34). Our results indicate that, during tumor progression, lung cancer cells take advantage of the ability of p38α to regulate targets like TIMP-1, a metalloproteinase inhibitor that not only regulates extracellular matrix catabolism but also promotes cell proliferation and survival in an autocrine manner. This latter function of TIMP-1 is based on both the regulation of the pericellular availability of protease-dependent growth factor or cytokine signals and the binding to CD44/pro-MMP9 or to CD63, which in turn can stimulate ERK, FAK,

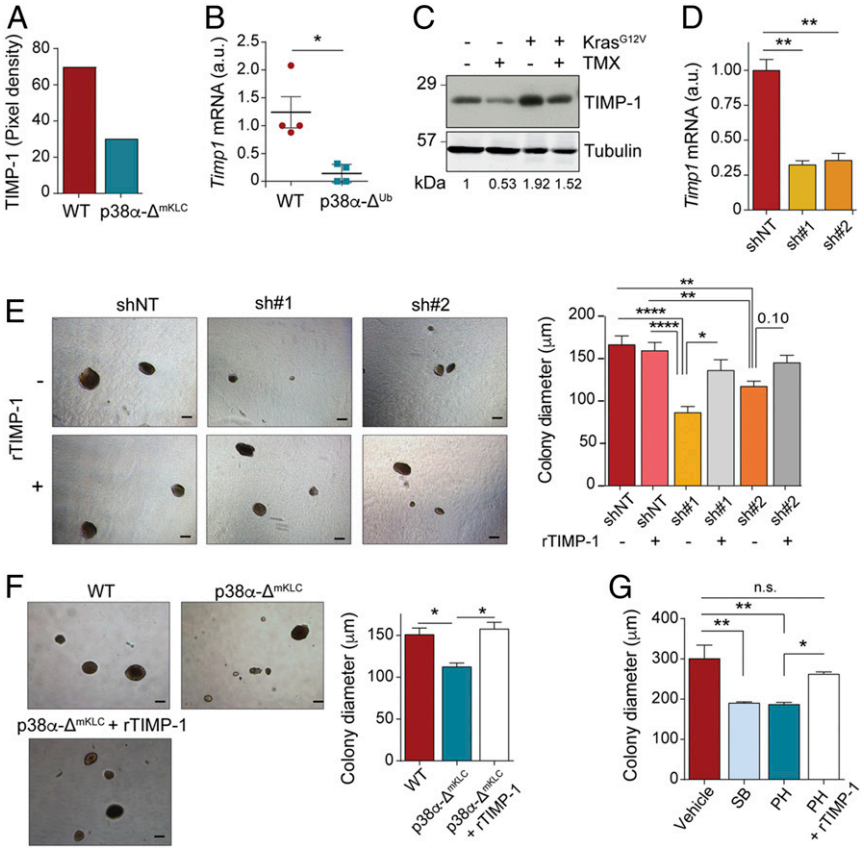

Fig. 6. p38α-regulated expression of TIMP-1 induces lung cancer cell proliferation. (*A*) Relative TIMP-1 protein levels in lung tumors from mice that were intratracheally inoculated with either WT or p38α-Δ^{mKLC} cells, as determined using a cytokine array ($n = 20$ tumors from 4 mice per condition analyzed in a single array). (*B*) Relative *Timp1* mRNA expression in tumors from WT and p38α-Δ^{Ub} mice ($n = 4$ tumors from ≥3 mice per group). (*C*) Representative immunoblots with antibodies to TIMP-1 and tubulin as a loading control of whole lung lysates from WT and p38α-Δ^{Ub} mice, as indicated by − and + tamoxifen (TMX), respectively, either expressing or not expressing the *Kras^{G12V}* oncogene. Each line corresponds to one mouse. (*D*) Histogram showing *Timp1* down-regulation in WT mKLC cells treated with shRNAs targeting *Timp1* (sh#1 and sh#2) or a nontargeting control (shNT). (*E*) Representative images of the soft agar colonies formed by WT mKLC cells treated as in *D* in the presence or absence of recombinant TIMP-1 protein (rTIMP-1; 0.1 μg/mL) added twice per week. (Scale bars, 150 μm.) The histogram shows the average colony diameters ($n \geq 52$ colonies analyzed per group from 3 replicates). (*F*) Representative images of the soft agar colonies formed by WT cells, p38α-Δ^{mKLC} cells, and p38α-Δ^{mKLC} cells treated with rTIMP-1 protein (0.1 μg/mL) twice per week. (Scale bars, 150 μm.) The histogram shows the average colony diameters ($n \geq 144$ colonies analyzed per group from 6 replicates). (*G*) Average diameters of the colonies formed by the human NSCLC cell line H460 grown in soft agar for 20 d and treated with vehicle, the p38α inhibitors SB203580 (SB) and PH797804 (PH), or PH plus 0.1 μg/mL rTIMP-1 protein (≥119 colonies analyzed per group from 3 replicates). Data represent mean ± SEM. $*P < 0.05$, $**P < 0.01$, $****P < 0.0001$. n.s., not significant.

YAP/TAZ, and PI3K signaling pathways (35, 36). Accordingly, clinical studies have positively correlated high Timp-1 expression levels with poor prognosis in lung and colon cancer patients, as well as with short relapse time and advanced-stage tumors from breast and brain origin (37).

It has been reported that the IKK2/NFκB and p38 MAPK/ATF-2 pathways can both induce *Timp1* transcription in IL-1–stimulated human astrocytes, consistent with the presence of AP-1, NFκB, and ATF-2 binding sites on the *Timp1* promoter (30). A previous study also showed that IKK2 down-regulation decreases tumor cell proliferation in a mouse model of lung cancer, which correlates with decreased expression of TIMP-1 (27), mirroring the phenotype of p38α down-regulation. Here we show that chemical inhibition of either p38α or IKK2 impairs the proliferation of epithelial lung cancer cells in soft agar. Of note, p38α and NFκB can coordinately control the expression of several genes, such as the CXCL10 cytokine (38, 39), which we also found down-regulated in p38α-deficient lung tumors. In fact, p38α has been reported to target IκB for degradation (40) and to modulate the acetylation of p65, hence controlling the transcriptional activity of NFκB (41). Therefore, it seems likely that both pathways might perform overlapping functions in lung tumor progression. It would be interesting to test whether the combined inhibition of p38α and IKK2 could prevent any compensatory cross-talk and suffice to trigger lung tumor regression instead of the cytostatic effect observed upon inhibition of either single pathway alone.

Our studies identify p38α as a synthetic lethal interactor of Kras^{G12V} in lung epithelial cancer cells, suggesting its potential interest as a therapeutic target. As proof of concept, we used the p38α pharmacological inhibitor PH797804 that reached phase II clinical trials for chronic obstructive pulmonary disease (42). Treatment with PH797804 showed that p38α activity is required for the progression of genetically induced lung tumors to advanced stages. In addition, orthotopic xenograft experiments indicated that epithelial cancer cells rely on p38α signaling to proliferate within the pulmonary niche in vivo. Although metastatic properties of lung cancer cells do not seem to depend on p38α, our results indicate that the malignancy and size of the lung tumor mass is ultimately determined by the epithelial p38α levels. This dependency on p38α is highlighted by the anchorage-independent proliferation assays using lung epithelial cancer cells ex vivo, and agrees with a report of signet-ring carcinoma cell lines that also form smaller colonies when treated with the p38 MAPK inhibitor SB203580 (43). Taken together, our data

indicate a protumorigenic function of p38α in epithelial cancer cells of KRAS-driven lung tumors.

There is evidence that p38α can also mediate noncancer cell-autonomous functions in lung tumors. Ubiquitous expression of a nonphosphorylatable p38α mutant has been reported to impair the synthesis of hyaluronic acid by cancer-associated fibroblasts, reducing lung cancer cell proliferation (21). p38α can also regulate PD-L1 expression in $Kras^{G12V}$-driven cancer cells, thus impairing the tumor immunosurveillance capacity (44). Moreover, p38α might control the ability of infiltrating myeloid cells to contribute to lung adenocarcinoma progression, as described in colon cancer via IGF1 production (45). Therefore, p38α seems to control the production of different extracellular factors that will build autocrine and reciprocal signaling circuitries between stromal and cancer cells, in a way comparable to the circuitry established by human lung stem cells and their niche (46). These results support the use of pharmacological inhibitors of p38α to target protumorigenic functions of both cancer cells and stromal cells in lung tumors.

Whether the dependency on p38α for lung tumor progression is restricted to KRAS mutant tumors or applies to other lung tumors independently of the driver mutation remains to be investigated. In the case of lung tumors with nonfunctional p53, which account for about half of NSCLC cases (47), it has been reported that mice systemically expressing nonphosphorylatable p38α show decreased $Kras^{G12D}$-induced tumor burden (21). Moreover, our results using the human cancer cell lines H460 ($p53^{wt}$) and H358 (p53-deleted) suggest that epithelial p38α facilitates soft-agar growth independently of the p53 status. It should be also noted that p38α has been reported to facilitate resistance of lung tumors to cisplatin in vivo in both p53-proficient and -deficient mouse models (48, 49). Therefore, the requirement for p38α signaling in cancer cell fitness and in its interaction with the stroma is likely to represent a selective difference between normal cells and cancer cells in different tumor types, which can be exploited to treat lung adenocarcinoma and perhaps to improve the efficacy of currently used drugs.

Methods

Mice. $Kras^{+/FSFG12V}$ mice (23) were crossed with $Mapk14^{lox/lox}$ (9, 50), $Mapk14^{+/-}$ (51), and UBC-Cre-ERT2 mice (52) to obtain the genotypes $Mapk14^{lox/lox}$;Ub-CreERT2;$Kras^{+/FSFG12V}$ and $Mapk14^{lox/-}$;Ub-CreERT2;$Kras^{+/FSFG12V}$, which both gave indistinguishable phenotypes. $Kras^{+/FSFG12V}Mapk14^{lox/lox}$ mice were alternatively crossed to Sftpc-Cre-ER mice (53) to obtain mice with lung-specific p38α down-regulation (p38α-Δ^{SPC}). The two p38α-deficient mouse lines were on a mixed C57BL/6-FVB background and showed indistinguishable lung phenotypes, as determined by histology studies. Littermate controls of both sexes were used in all experiments. Mice were housed according to the national and European Union regulations, and protocols were approved by the animal care and use committees of both the Barcelona Science Park (PCB) and Biomedical Research Park of Barcelona (PRBB).

Generation of mKLC Cells and p38α Down-Regulation Ex Vivo. Primary adenocarcinomas generated in $Mapk14^{lox/lox}$;$Kras^{+/FSFG12V}$ mice were orthotopically implanted in Crl:NU-Foxn1nu mice as previously described (26). A freshly collected fragment of lung tumor was minced with sterile scalpels and then plated in Dulbecco's modified Eagle medium (DMEM) supplemented with 20% fetal bovine serum (FBS) plus 1% penicillin/streptomycin. Medium was renewed once per week until colonies with epithelial cell morphology were observed. Then, cells were trypsinized and expanded as established cell lines.

To down-regulate p38α, mKLC cells with $Mapk14^{lox/lox}$ alleles were treated with Tat-Cre recombinant protein (54) at a concentration of 150 μg/mL in serum-free DMEM with 1% penicillin/streptomycin. After 10 h, medium was replaced with DMEM 10% FBS, and cells were passaged twice before performing experiments. For mKLC cells carrying both $Mapk14^{lox/lox}$ alleles and inducible Cre-ERT2, p38α down-regulation was induced by treating with 4OH-TMX (10 μM; Sigma H6278) for 3 d.

Orthotopic Implantation. Immunocompetent mice were anesthetized and intratracheally inoculated with 100 μL of a 2×10^6 mKLC cells per milliliter solution, and tumors were left to grow for 25 d. For intratracheal administration, cells were cultured to 70% confluence in DMEM 10% FBS, diluted with PBS, kept on ice, and thoroughly mixed prior to each inoculation. The vocal cords were viewed directly with the help of a cold light source, and a blunted catheter coupled to a syringe was passed beyond them to inoculate the cells.

Histopathological Analysis and Immunohistochemistry. Mouse lungs were fixed by insufflating 10% neutral buffered formalin (Sigma) through the trachea with a syringe, incubated overnight at 4 °C in 10 mL 10% neutral buffered formalin, and then embedded in paraffin. Tumors in freshly harvested lungs were counted and sized, and lung sections stained with hematoxylin and eosin (H&E) were analyzed for tumor grade by two independent observers in a blinded fashion. Tumor grade was evaluated following established classifications (55). The human lung cancer tissue array (US Biomax; HLug-Ade050CD-01) included lung adenocarcinoma samples with adjacent normal tissues and samples of normal lung from patients without tumor. After staining, it was evaluated blindly by three independent observers. Slides were incubated using the following antibodies: CD31 (Abcam no. 28364; 1:500), CD45 (BD Biosciences no. 550539; 1:100), CD68 (Biorbyt no. 47985; 1:750), cleaved caspase-3 (Cell Signaling no. 9661; 1:500), Ki67 (Novocastra no. NCL-Ki67p; 1:500), p38α (Cell Signaling no. 9218; 1:50), phospho-Thr180/Tyr182 p38 MAPK (Cell Signaling no. 4631; 1:50), phospho-Thr334 MK2 (Cell Signaling no. 3007; 1:100), phospho-Tyr705 STAT3 (Cell Signaling no. 9145S; 1:200), pro-SPC (Millipore no. AB3786; 1:3,000), and HRP-conjugated secondaries (ImmunoLogic and Dako). Immunostaining was visualized with 3,3-diaminobenzidine and counterstained with hematoxylin or subsequently incubated with Alexa-conjugated secondary antibodies (Life Technologies A21441; 1:400). To detect apoptosis in paraffin-embedded samples, the fluorescein in situ cell death detection kit (Roche no. 11684795910) was used according to the manufacturer's instructions.

Whole digital slides were acquired with a slide scanner (NanoZoomer; Hamamatsu), and individual images were captured with NDP view software. All tumors in each tissue section were analyzed. Positive signals were quantified in an automated manner based on either the relative percentage of stained surface in a tumor or the relative percentage of positive cells per tumor using computerized imaging software (ImageJ).

Statistical Methods. Data are presented as means ± SEM unless otherwise indicated. Dataset statistics were analyzed with Prism 7 (GraphPad Software). Groups were compared using the two-tailed Mann–Whitney test or analysis of variance (ANOVA; Kruskal–Wallis). *P* values smaller than 0.05 were considered statistically significant.

Data Availability. All relevant data, associated protocols, and materials are within the manuscript and its *SI Appendix*. Any additional information needed will be available upon request from the corresponding author.

ACKNOWLEDGMENTS. We thank M. Onaitis for kindly providing the SPC-Cre mouse, E. Brown for UBC-Cre-ERT2 mice, M. Pasparakis for the plasmid to express Tat-Cre protein, and A. Igea for the purified Tat-Cre protein. We acknowledge the technical assistance of August Vidal from Hospital Universitari de Bellvitge; Neus Prats and the Institute for Research in Biomedicine (IRB) Histology facility members; Camille Stephan-Otto Attolini and Oscar Reina from the IRB Biostatistics/Bioinformatics facility; the IRB Genomics Unit; and Jaume Comas and the Universitat de Barcelona (UB) Fluorescence-Activated Cell Sorting facility members. We are grateful to Sara Mainardi and Carmen Guerra for insights into lung tumor histopathology; Jordi Hernández, Raquel Batlle, Antonio Maraver, David Santamaria, Chiara Ambrogio, and Monica Cubillos-Rojas for helpful suggestions and support; and Ivan del Barco for input early in the project. This work was supported by grants from the European Research Council (ERC 294665), Ministerio de Ciencia, Innovación y Universidades (MICINN) (BFU2010-17850 and SAF2016-81043-R), Agència de Gestió D'Ajuts Universitaris I de Recerca (AGAUR) (2017 SRG-557), and Fundación Banco Bilbao Vizcaya Argentaria (BBVA). J.V.F. acknowledges a Formación de Personal Investigador (FPI) predoctoral fellowship. IRB Barcelona is the recipient of institutional funding from MICINN through the Centres of Excellence Severo Ochoa award and from the Centres de Recerca de Catalunya (CERCA) Program of the Catalan Government.

1. W. D. Travis *et al.*; WHO Panel, The 2015 World Health Organization classification of lung tumors: Impact of genetic, clinical and radiologic advances since the 2004 classification. *J. Thorac. Oncol.* **10**, 1243–1260 (2015).
2. L. Bombardelli, A. Berns, The steady progress of targeted therapies, promising advances for lung cancer. *Ecancermedicalscience* **10**, 638 (2016).
3. R. B. Blasco *et al.*, c-Raf, but not B-Raf, is essential for development of K-Ras oncogene-driven non-small cell lung carcinoma. *Cancer Cell* **19**, 652–663 (2011).
4. R. Nagel, E. A. Semenova, A. Berns, Drugging the addict: Non-oncogene addiction as a target for cancer therapy. *EMBO Rep.* **17**, 1516–1531 (2016).

5. M. S. Kumar *et al*., The GATA2 transcriptional network is requisite for RAS oncogene-driven non-small cell lung cancer. *Cell* **149**, 642–655 (2012).
6. A. Cuenda, S. Rousseau, p38 MAP-kinases pathway regulation, function and role in human diseases. *Biochim. Biophys. Acta* **1773**, 1358–1375 (2007).
7. A. Cuadrado, A. R. Nebreda, Mechanisms and functions of p38 MAPK signalling. *Biochem. J.* **429**, 403–417 (2010).
8. L. Hui *et al*., p38alpha suppresses normal and cancer cell proliferation by antagonizing the JNK-c-Jun pathway. *Nat. Genet.* **39**, 741–749 (2007).
9. J. J. Ventura *et al*., p38alpha MAP kinase is essential in lung stem and progenitor cell proliferation and differentiation. *Nat. Genet.* **39**, 750–758 (2007).
10. J. Gupta *et al*., Dual function of p38α MAPK in colon cancer: Suppression of colitis-associated tumor initiation but requirement for cancer cell survival. *Cancer Cell* **25**, 484–500 (2014).
11. E. F. Wagner, A. R. Nebreda, Signal integration by JNK and p38 MAPK pathways in cancer development. *Nat. Rev. Cancer* **9**, 537–549 (2009).
12. K. Leelahavanichkul *et al*., A role for p38 MAPK in head and neck cancer cell growth and tumor-induced angiogenesis and lymphangiogenesis. *Mol. Oncol.* **8**, 105–118 (2014).
13. B. Gil-Araujo *et al*., Dual specificity phosphatase 1 expression inversely correlates with NF-κB activity and expression in prostate cancer and promotes apoptosis through a p38 MAPK dependent mechanism. *Mol. Oncol.* **8**, 27–38 (2014).
14. A. K. Greenberg *et al*., Selective p38 activation in human non-small cell lung cancer. *Am. J. Respir. Cell Mol. Biol.* **26**, 558–564 (2002).
15. G. Mountzios *et al*., Mitogen-activated protein kinase activation in lung adenocarcinoma: A comparative study between ever smokers and never smokers. *Clin. Cancer Res.* **14**, 4096–4102 (2008).
16. K. Rikova *et al*., Global survey of phosphotyrosine signaling identifies oncogenic kinases in lung cancer. *Cell* **131**, 1190–1203 (2007).
17. K. Liu *et al*., Sunlight UV-induced skin cancer relies upon activation of the p38α signaling pathway. *Cancer Res.* **73**, 2181–2188 (2013).
18. H. Zheng *et al*., A posttranslational modification cascade involving p38, Tip60, and PRAK mediates oncogene-induced senescence. *Mol. Cell* **50**, 699–710 (2013).
19. M. Korc, p38 MAPK in pancreatic cancer: Finding a protective needle in the haystack. *Clin. Cancer Res.* **20**, 5866–5868 (2014).
20. M. S. Alam *et al*., Selective inhibition of the p38 alternative activation pathway in infiltrating T cells inhibits pancreatic cancer progression. *Nat. Med.* **21**, 1337–1343 (2015).
21. A. Brichkina *et al*., p38MAPK builds a hyaluronan cancer niche to drive lung tumorigenesis. *Genes Dev.* **30**, 2623–2636 (2016).
22. Y. Matsuo *et al*., Involvement of p38alpha mitogen-activated protein kinase in lung metastasis of tumor cells. *J. Biol. Chem.* **281**, 36767–36775 (2006).
23. M. Sanclemente *et al*., c-RAF ablation induces regression of advanced Kras/Trp53 mutant lung adenocarcinomas by a mechanism independent of MAPK signaling. *Cancer Cell* **33**, 217–228.e4 (2018).
24. S. Mainardi *et al*., Identification of cancer initiating cells in K-Ras driven lung adenocarcinoma. *Proc. Natl. Acad. Sci. U.S.A.* **111**, 255–260 (2014).
25. K. D. Sutherland *et al*., Multiple cells-of-origin of mutant K-Ras-induced mouse lung adenocarcinoma. *Proc. Natl. Acad. Sci. U.S.A.* **111**, 4952–4957 (2014).
26. C. Ambrogio *et al*., Modeling lung cancer evolution and preclinical response by orthotopic mouse allografts. *Cancer Res.* **74**, 5978–5988 (2014).
27. Y. Xia *et al*., Reduced cell proliferation by IKK2 depletion in a mouse lung-cancer model. *Nat. Cell Biol.* **14**, 257–265 (2012).
28. I. S. Aljada *et al*., Upregulation of the tissue inhibitor of metalloproteinase-1 protein is associated with progression of human non-small-cell lung cancer. *J. Clin. Oncol.* **22**, 3218–3229 (2004).
29. M. Pesta *et al*., Prognostic significance of TIMP-1 in non-small cell lung cancer. *Anticancer Res.* **31**, 4031–4038 (2011).
30. K. M. Wilczynska *et al*., A novel mechanism of tissue inhibitor of metalloproteinases-1 activation by interleukin-1 in primary human astrocytes. *J. Biol. Chem.* **281**, 34955–34964 (2006).
31. A. Igea, A. R. Nebreda, The stress kinase p38α as a target for cancer therapy. *Cancer Res.* **75**, 3997–4002 (2015).
32. W. Wang *et al*., Sequential activation of the MEK-extracellular signal-regulated kinase and MKK3/6-p38 mitogen-activated protein kinase pathways mediates oncogenic ras-induced premature senescence. *Mol. Cell. Biol.* **22**, 3389–3403 (2002).
33. A. Freund, C. K. Patil, J. Campisi, p38MAPK is a novel DNA damage response-independent regulator of the senescence-associated secretory phenotype. *EMBO J.* **30**, 1536–1548 (2011).
34. X. J. Fan *et al*., Phosphorylated p38, a negative prognostic biomarker, complements TNM staging prognostication in colorectal cancer. *Tumour Biol.* **35**, 10487–10495 (2014).
35. B. Grünwald, B. Schoeps, A. Krüger, Recognizing the molecular multifunctionality and interactome of TIMP-1. *Trends Cell Biol.* **29**, 6–19 (2019).
36. T. Ando *et al*., Tissue inhibitor of metalloproteinase-1 promotes cell proliferation through YAP/TAZ activation in cancer. *Oncogene* **37**, 263–270 (2018).
37. H. W. Jackson, V. Defamie, P. Waterhouse, R. Khokha, TIMPs: Versatile extracellular regulators in cancer. *Nat. Rev. Cancer* **17**, 38–53 (2017).
38. S. Saccani, S. Pantano, G. Natoli, p38-Dependent marking of inflammatory genes for increased NF-kappa B recruitment. *Nat. Immunol.* **3**, 69–75 (2002).
39. C. K. Wong, C. B. Wang, W. K. Ip, Y. P. Tian, C. W. Lam, Role of p38 MAPK and NF-kB for chemokine release in coculture of human eosinophils and bronchial epithelial cells. *Clin. Exp. Immunol.* **139**, 90–100 (2005).
40. P. Viatour, M. P. Merville, V. Bours, A. Chariot, Phosphorylation of NF-kappaB and IkappaB proteins: Implications in cancer and inflammation. *Trends Biochem. Sci.* **30**, 43–52 (2005).
41. R. N. Saha, M. Jana, K. Pahan, MAPK p38 regulates transcriptional activity of NF-kappaB in primary human astrocytes via acetylation of p65. *J. Immunol.* **179**, 7101–7109 (2007).
42. W. MacNee, R. J. Allan, I. Jones, M. C. De Salvo, L. F. Tan, Efficacy and safety of the oral p38 inhibitor PH-797804 in chronic obstructive pulmonary disease: A randomised clinical trial. *Thorax* **68**, 738–745 (2013).
43. Q. Xu *et al*., The PI 3-kinase-Rac-p38 MAP kinase pathway is involved in the formation of signet-ring cell carcinoma. *Oncogene* **22**, 5537–5544 (2003).
44. M. A. Coelho *et al*., Oncogenic RAS signaling promotes tumor immunoresistance by stabilizing PD-L1 mRNA. *Immunity* **47**, 1083–1099.e6 (2017).
45. C. Youssif *et al*., Myeloid p38α signaling promotes intestinal IGF-1 production and inflammation-associated tumorigenesis. *EMBO Mol. Med.* **10**, e8403 (2018).
46. E. J. Ruiz, F. Oeztuerk-Winder, J. J. Ventura, A paracrine network regulates the cross-talk between human lung stem cells and the stroma. *Nat. Commun.* **5**, 3175 (2014).
47. Z. Chen, C. M. Fillmore, P. S. Hammerman, C. F. Kim, K. K. Wong, Non-small-cell lung cancers: A heterogeneous set of diseases. *Nat. Rev. Cancer* **14**, 535–546 (2014).
48. S. Morandell *et al*., A reversible gene-targeting strategy identifies synthetic lethal interactions between MK2 and p53 in the DNA damage response in vivo. *Cell Rep.* **5**, 868–877 (2013).
49. A. Brichkina *et al*., Proline isomerisation as a novel regulatory mechanism for p38MAPK activation and functions. *Cell Death Differ.* **23**, 1592–1601 (2016).
50. J. Heinrichsdorff, T. Luedde, E. Perdiguero, A. R. Nebreda, M. Pasparakis, p38 alpha MAPK inhibits JNK activation and collaborates with IkappaB kinase 2 to prevent endotoxin-induced liver failure. *EMBO Rep.* **9**, 1048–1054 (2008).
51. R. H. Adams *et al*., Essential role of p38alpha MAP kinase in placental but not embryonic cardiovascular development. *Mol. Cell* **6**, 109–116 (2000).
52. Y. Ruzankina *et al*., Deletion of the developmentally essential gene ATR in adult mice leads to age-related phenotypes and stem cell loss. *Cell Stem Cell* **1**, 113–126 (2007).
53. X. Xu *et al*., Evidence for type II cells as cells of origin of K-Ras-induced distal lung adenocarcinoma. *Proc. Natl. Acad. Sci. U.S.A.* **109**, 4910–4915 (2012).
54. M. Peitz, K. Pfannkuche, K. Rajewsky, F. Edenhofer, Ability of the hydrophobic FGF and basic TAT peptides to promote cellular uptake of recombinant Cre recombinase: A tool for efficient genetic engineering of mammalian genomes. *Proc. Natl. Acad. Sci. U.S.A.* **99**, 4489–4494 (2002).
55. E. L. Jackson *et al*., Analysis of lung tumor initiation and progression using conditional expression of oncogenic K-ras. *Genes Dev.* **15**, 3243–3248 (2001).